# Complexation between *tert*-Butyl Ketones and *β*-Cyclodextrin. Structural Study by NMR and MD Simulations

Mariluz Zubiaur and Carlos Jaime*

*Departament de Química, Universitat Autònoma de Barcelona, 08193 Bellaterra (Barcelona), Spain*

*carlos.jaime@uab.es*

*Received April 19, 2000*

A structural study (NMR and MD) of the complexation between *tert*-butyl ketones and *β*-cyclodextrin has been performed. A priority order for the alkyl and phenyl groups composing the ketones has been determined based on association constants: Ph- > $C_6H_{11}$- = *t*-Bu- > Bu-, Pr-, Me-. Geometries for the complexes are proposed based on NOE values and on the MD simulations. Bimodal complexation occurs in all the compounds studied.

## Introduction

Cyclodextrins (CyDs) are cyclic oligosaccharides formed by units (six, seven, or eight) of α-D-(+)-glucopyranose called α-, *β*- or *γ*-CyD, respectively. Their structure provides them with toroidal shape with an inner low polar cavity, which allows them to include a big variety of organic molecules.[1−3] The formation of host/guest complexes has been used in industry to increase bioavailability, taste, and stability of drugs in aqueous solution.[4] They have also been used as enzyme models.[5,6] A variety of techniques are available to observe host/guest interactions depending on the applications envisaged for the complex.[7] However, most of these techniques are unable to discriminate between internal (inclusion) and external complexation.

The assessment of a priority order for functional groups is the aim of researchers in many fields of chemistry, and the study of the preference for inclusion in the cavity of CyDs has also been the subject of several studies.[8,9] The facility with which the *tert*-butyl group is included in the *γ*-CyD has been shown by ESR experiments.[8] The inclusion is preferred to that of alkyl chains, similar to that of the phenyl ring, and less than that for the cyclohexane ring.

In this article a structural study of the complexes between five *tert*-butyl ketones, **1**−**5**, and *β*-CyD has been carried out by means of NMR spectroscopy and molecular dynamics simulations. The aim of this study is as follows: (i) to determine a priority order for standard functional groups when complexing with *β*-CyD, probably the most widely used CyD in aqueous solution, and (ii) to identify the most probable geometry for the inclusion.

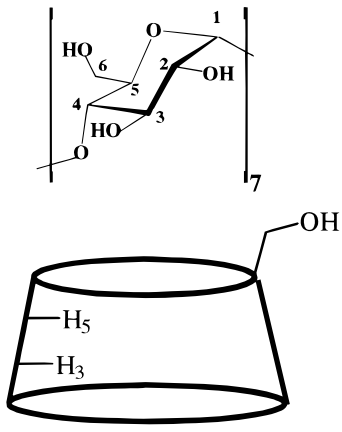


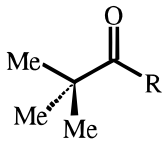


**1,** R = Ph
**2,** R = Me
**3,** R = Pr
**4,** R = Bu
**5,** R = $C_6H_{11}$

**α-CyD**: 6 glucose units
**β-CyD**: 7 glucose units
**γ-CyD**: 8 glucose units

All substrates have two well-delimited functional groups separated by one carbonyl group. Consequently, bimodality can occur, and the formation of two different inclusion complexes **A** and **B** (Figure 1) has been considered throughout the study.

## Results

**NMR Experiments.** Internal *β*-CyD protons ($H_{3'}$ and $H_{5'}$) and guest protons suffer from large induced chemical shifts when the host/guest ratio changes, denoting the formation of an inclusion complex. Figure 2 contains partial NMR spectra for the **1**/*β*-CyD complex as an example. Information on the stoichiometry and formation constant can be extracted by adjusting the data to the variation of the chemical shifts for protons involved in the complexation.[10] Table 1 contains the information for the **1**/*β*-CyD complex also as an example.

(1) Pringsheim, H.; Lirchtenstein, S. *Ber.* **1916**, *49*, 364.
(2) Freudenberg, K.; Cramer, F.; *Z. Naturforsch.* **1948**, *B3*, 464.
(3) An excellent and recent review is the special number of *Chem. Rev.*: D'Souza, V. T., Lipkowitz, K. (guests editors) *Chem. Rev.* **1998**, *98,* all pages.
(4) Saenger, W. *Angew. Chem., Int. Ed. Engl.* **1980**, *19*, 344, and references therein.
(5) Bender, M.; Komiyama L. *Cyclodextrin Chemistry*; Springer: Berlin, 1978.
(6) Vögtle, F. *Supramolecular Chemistry: an Introduction*; John Wiley & Sons Ltd.: New York, 1991.
(7) Higuchi, T.; Connors, K. A. *Adv. Anal. Chem. Instr.* **1965**, *4*, 117.
(8) (a) Kotake, Y.; Janzen, E. G. *J. Am. Chem. Soc.* **1989**, *111*, 2066, 5138, and 7319. (b) Kotake, Y.; Janzen, E. G. *J. Am. Chem. Soc.* **1992**, *114*, 2872.
(9) (a) Tee, O. S.; Mazza, C.; Du, X.-X. *J. Org. Chem.* **1990**, *55*, 3603. (b) Gadosy, T. A.; Tee, O. S. *J. Chem. Soc., Perkin Trans. 2* **1994**, 715. (c) Tee, O. S.; Gadosy, T. A.; Giorgi, J. B. *J. Chem. Soc., Perkin Trans. 2* **1994**, 2191. (d) Tee, O. S.; Gadosy, T. A.; Giorgi, J. B. *J. Chem. Soc., Perkin Trans. 2* **1995**, 71. (e) Tee, O. S.; Du, X. X. *J. Am. Chem. Soc.* **1992**, *114*, 620. (f) Tee, O. S.; Bozzi, M.; Hoeven, J. J.; Gadosy, T. A. *J. Am. Chem. Soc.* **1993**, *115*, 8990. (g) Tee, O. S.; Mazza, C.; Lozano-Hemmer, R.; Giorgi, J. B. *J. Org. Chem.*, **1994**, *59*, 7602. (h) Tee, O. S.; Gadosy, T. A.; *J. Chem. Soc., Perkin Trans. 2*, **1994**, *11*, 2307.
(10) (a) Hynes, M. J. *J. Chem. Soc., Dalton Trans.* **1993**, 311. (b) Barrans, R. E.; Dougherty, D. A. *Supramol. Chem.* **1994**, *4*, 121. (c) Salvatierra, D.; Díez, C.; Jaime, C. *J. Inclusion Phenom.* **1997**, *27*, 215.

10.1021/jo0006021 CCC: $19.00 
Published on Web 10/27/2000

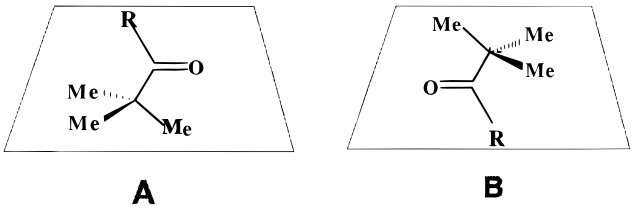


**Figure 1.** Scheme of the two possible orientations for an inclusion complex (bimodality).

The stoichiometry of the complex can be determined by using the Job method[11] if the [host] + [guest] is constant. As a consequence of the solubility of the different guests used, the Job method has been applied in just one case (pinacolone, **2**). Although less precisely, the stoichiometry for all other complexes were determined by graphical representation of the induced chemical shifts, $\Delta\delta_A$, versus the host/guest ratio [B]/[A]. Figure 3 shows that both methods indicate a 1:1 stoichiometry for the **2**/$\beta$-CyD complex.

2D-ROESY experiments were carried out on samples having *host/guest* or *guest/host* ratios higher than 1.5 to shift the equilibrium toward the formation of the complex but ensuring detectable species signals. NOE values were qualitatively used; no quantitative conclusions on intermolecular distances were extracted due to the large dynamics in the complexation process. Table 2 contains all NOE values for the complexes studied. Protons for the R group are labeled depending on their position relative to the CO group. Experimental NOE values were divided by the number of protons responsible for the signal to obtain comparable values. On-resonance ROE methods give false NOE signals between guest and external host protons, while off-resonance methods[12] did not (see the Experimental Section for details).

***tert*-Butyl Phenyl Ketone/$\beta$-CyD Complex, 1/$\beta$-CyD.** Study of its NMR spectra through the variation of the $\delta$ for the inner ($H_{3'}$, and $H_{5'}$) $\beta$-CyD protons (Figure 4a) reveals the formation of an inclusion complex with 1:1 host/guest stoichiometry. When the external protons ($H_{2'}$ and $H_{4'}$) were studied, a reasonable plot was obtained although induced shifts were 10 times smaller (Figure 4b). Two possibilities may justify these induced shifts: magnetic anisotropy caused by functional groups, and formation of external complexation, also with 1:1 host/guest stoichiometry. The complexation constant magnitude can be deduced from the form of the $\Delta\delta_A$ vs [host]/[guest] or [guest]/[host] graphs (large if the plateau is achieved early). Comparison of plots for the internal and external protons (Figure 4) indicates that internal and external (if any) complexation constants should have similar values.

The sample used for the 2D-ROESY experiments gave two sets of signals for the guest protons (Figure 5); positive NOE signals appear between the two (Figure 5a) indicating chemical exchange. The signals with better resolution present negative NOE signals with the $\beta$-CyD protons (Figure 5b), thus corresponding to the complexed species, while the worse resolved signals do not present intermolecular NOEs and thus correspond to the free species. This implies slower complexation than the rest of the compounds studied.

The simultaneous presence of NOE for the pairs $H_p/H_{3'}$ and $H_{t-Bu}/H_{3'}$ (Table 2) indicates two possible geometries, **A** and **B**, for the inclusion complex. Moreover, the larger NOE values between aromatic protons and $H_{5'}$ than those with $H_{3'}$ suggest that the aromatic ring is nearer to primary hydroxyl groups than to the *tert*-butyl group (complex of type **A**). Consistent with this observation, the NOE value for the $H_{t-Bu}/H_{3'}$ pair is also greater than that for the $H_{t-Bu}/H_{5'}$ pair, suggesting the preference of the *t*-Bu group for the wider part of the cavity (complex of type **A**).

**Pinacolone/$\beta$-CyD Complex, 2/$\beta$-CyD.** The NMR study (Figure 2) indicates the formation of inclusion complex with 1:1 host/guest stoichiometry. External $\beta$-CyD protons ($H_{2'}$ but not $H_{4'}$) present reasonable correlation curves for $\Delta\delta_A$ vs [**2**]/[$\beta$-CyD], but their Job diagrams are not symmetrical. In contrast, guest protons give good curves with symmetrical Job diagrams. All these facts may be attributed to a larger preference for the internal over a possible external complexation. In contrast, the off-resonance 2D-ROESY experiments indicate the presence of an exclusive internal complexation. NOE effects (Table 2) again suggest two possible geometries for the inclusion complex, **A** and **B**, without preference for any group inclusion, although both groups are nearer to $H_{3'}$ than to $H_{5'}$, i.e., they prefer the wider part of the cavity.

***tert*-Butyl Propyl Ketone/$\beta$-CyD, 3/$\beta$-CyD.** A 1:1 host/guest stoichiometry was deduced for this inclusion complex. The external $\beta$-CyD protons ($H_{4'}$ but not $H_{2'}$) give reasonable plots for $\Delta\delta_A$ vs [**3**]/[$\beta$-CyD] although they achieve the plateau more slowly than the internal protons. Guest protons produce single plots for their induced $\delta$. These facts are compatible with an inclusion preferred over a possible external complexation because induced shifts produced by the internal complexation hide those coming from the external complexation. Results from off-resonance 2D-ROESY experiments are justified on the basis of an internal association. Observed NOE effects (Table 2) suggest two possible geometries for the inclusion complex. NOE values over $H_{3'}$ are larger than those over $H_{5'}$ for all protons, thus indicating preference for the wider half of the cavity. Ratios of NOE values $H_x\{H_{3'}\}/H_x\{H_{5'}\}$ indicate that the R group is closer to $H_{3'}$ than the *tert*-butyl (i.e. predominance of type **B** complex).

**Butyl *tert*-Butyl Ketone/$\beta$-CyD, 4/$\beta$-CyD.** NMR data indicate the formation of an inclusion complex with 1:1 host/guest stoichiometry. External $\beta$-CyD protons give good plots $\Delta\delta_A$ vs [**4**]/[$\beta$-CyD] although they reach the plateau more slowly than the internal. Guest protons also produce good single curves indicating the formation of a 1:1 complex, and suggesting an important internal complexation. Off-resonance 2D-ROESY experiments demonstrate again the presence of only internal complexation, although the results on Table 2 suggest two geometries for the inclusion complex. Nevertheless, the larger NOE values of the alkyl hydrogens than those of the *t*-Bu group indicate greater proximity of both internal protons to the alkyl chain than to the *t*-Bu group (complexes of type **A** and **B** simultaneously).

***tert*-Butyl Cyclohexyl Ketone/$\beta$-CyD, 5/$\beta$-CyD.** Analysis of NMR data indicates the formation of an inclusion complex with 1:1 host/guest stoichiometry.

(11) Job, P. *Ann. Chim.* **1928**, *9*, 113.

(12) (a) Desvaux, H.; Berthault, B.; Birlirakis, N.; Goldman, N.; Piotto, M. *J. Magn. Res. A* **1994**, *A 113*, 47. (b) Desvaux, H.; Berthault, B.; Birlirakis, N. *Chem. Phys. Lett.* **1995**, *233*, 545.

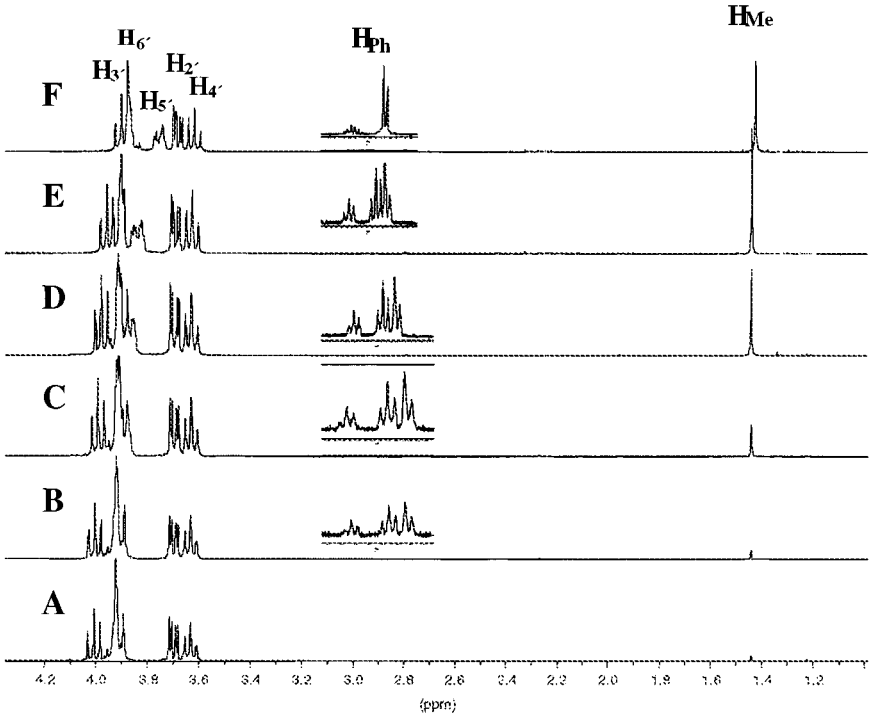


**Figure 2.** Partial 400 MHz $^1$H NMR spectra for host ($H_{3'}$, $H_{6'}$, $H_{5'}$, $H_{2'}$, and $H_{4'}$) and guest protons for solutions of the **1**/*β*-CyD complex with variable [host]/[guest] ratios. Values are: (A) 58.40; (B) 24.09, (C) 9.04; (D) 4.07, (E) 2.48, (F) 0.91.

**Table 1. Induced Chemical Shifts for Host ($H_{3'}$, $H_{5'}$, $H_{2'}$, and $H_{4'}$) and Guest ($H_{t-Bu}$, $H_p$, $H_o$, and $H_m$) Protons for the 14 Studied Samples of the 1/*β*-CyD Complex as an Example**

| sample | $\Delta\delta$ $H_p$ | $\Delta\delta$ $H_o$ | $\Delta\delta$ $H_m$ | $\Delta\delta$ $H_{t-Bu}$ | $\Delta\delta$ $H_{3'}$ | $\Delta\delta$ $H_{5'}$ | $\Delta\delta$ $H_{2'}$ | $\Delta\delta$ $H_{4'}$ |
|---|---|---|---|---|---|---|---|---|
| 1 | | | | 0.0311 | 0.0000 | 0.0000 | 0.0000 | 0.0000 |
| 2 | −0.0238 | 0.1977 | −0.0010 | 0.0311 | −0.0023 | −0.0030 | 0.0000 | 0.0000 |
| 3 | −0.0253 | 0.1948 | −0.0011 | 0.0319 | −0.0051 | −0.0073 | 0.0000 | 0.0007 |
| 4 | −0.0239 | 0.1915 | −0.0029 | 0.0344 | −0.0129 | −0.0202 | 0.0019 | 0.0019 |
| 5 | −0.0283 | 0.1838 | −0.0049 | 0.0370 | −0.0250 | −0.0389 | 0.0029 | 0.0036 |
| 6 | −0.0326 | 0.1728 | −0.0099 | 0.0399 | −0.0404 | −0.0623 | 0.0044 | 0.0058 |
| 7 | −0.0324 | 0.1194 | −0.0169 | 0.0392 | −0.0821 | −0.1290 | 0.0095 | 0.0115 |
| 8 | −0.0262 | 0.0867 | −0.0155 | 0.0304 | −0.0887 | −0.1408 | 0.0110 | 0.0132 |
| 9 | −0.0120 | 0.0488 | −0.0099 | 0.0180 | −0.0895 | −0.1422 | 0.0110 | 0.0132 |
| 10 | | | | | −0.0902 | −0.1431 | 0.0110 | 0.0132 |
| 11 | −0.0283 | 0.1109 | −0.0142 | 0.0348 | −0.0770 | −0.1225 | 0.0095 | 0.0110 |
| 12 | | | | | −0.0896 | −0.1431 | 0.0117 | 0.0139 |
| 13 | 0.0000 | 0.0000 | 0.0000 | 0.0000 | −0.0898 | −0.1419 | 0.0107 | 0.0129 |
| 14 | | | | | −0.0903 | −0.1416 | 0.0110 | 0.0132 |

Internal *β*-CyD, and guest protons gave excellent $\Delta\delta_A$ vs [**5**]/[*β*-CyD], and [*β*-CyD]/[**5**] plots, respectively. In contrast, external *β*-CyD protons ($H_{4'}$ but not $H_{2'}$) gave a plot for $\Delta\delta_A$ vs [**5**]/[ *β*-CyD] indicating that equilibrium was not achieved in the range of study (Figure 6). Comparison of all these plots suggests that the internal complexation was greater than the external. Off-resonance 2D-ROESY experiments for this complex also demonstrate that only internal complexation occurred. NOE values (Table 2) also suggest two simultaneous arrangements for the inclusion complex. The $H_{3'}$ is generally closer to the *tert*-butyl group than to the cyclohexyl, indicating preference for complex **A**.

**Determination of Association Constants.** This appears to be simple; however, when fast exchange occurs between two very distinct positions (complexed and free states) with different chemical shifts, the determination of the association constant based on the variation of the chemical shifts becomes difficult. The *δ* values of most protons change only slightly, which produces large errors in the association constants.

The association process is, in principle, unique; i.e., all the observed protons undergo the same association process (inclusion). Nevertheless, calculated association constants are different when different sets of protons are considered to evaluate K. Table 3 shows the association constants given by EQNMR program.[10a] This program considers a single proton for the calculation of K. In general, calculated K depends on the proton considered. However, K for compounds **1**−**5** is about $1.5 \times 10^4$, $2 \times 10^2$, $10^3$, $10^4$ and $10^4$, respectively.

A computer program has been developed in our laboratory (CALCK)[10c] which considers simultaneously the effect of all protons over the K., although the results are highly variable. When K is calculated considering all the protons convergence is not usually obtained. In most cases, convergence is obtained only when one or two protons are considered (Table 4). With this method, association Ks for compounds **1**−**5** are about $10^2$−$10^3$, $10^2$−$10^3$, $8 \times 10^3$, $5 \times 10^3$, and $10^3$, respectively. Compound **2** shows the lowest K with both methods.

The results obtained when using EQNMR are more coincident with the proposed order of preference for alkyl groups established by Kotake and Janzen.[8] We thus propose that *β*-CyD clearly prefers to complex molecules containing phenyl rings, closely followed by molecules containing cyclohexyl groups. No strong complexation of compounds **2** and **3** is deduced.

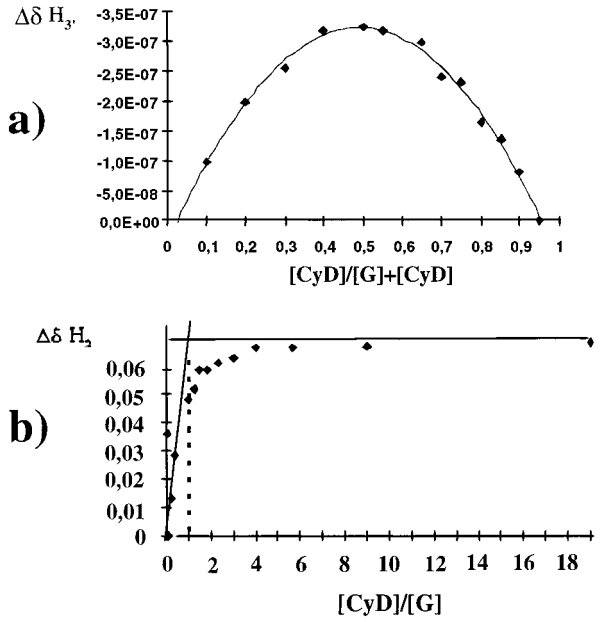


**Figure 3.** Analysis of NMR data for complex **1**/*β*-CyD: (a) Job's diagram for *β*-CyD $H_{3'}$ protons; (b) Plot of $\Delta\delta$ for the $H_{Me}$ guest protons vs [*β*-CyD]/[guest].

**Table 2. Observed NOE Values over All Studied Complexes (1-5/*β*-CyD) Obtained by Off-Resonance 2D-ROESY Methods**

| | | observed | |
|---|---|---|---|
| product | saturated | $7H_{3'}$- | $7H_{5'}$- |
| **1** | $H_{t-Bu}$ | 10.4 | 8.6 |
| | $H_p$ | 7.1 | 20.0 |
| | $H_o$ | 13.1 | 20.0 |
| | $H_m$ | 16.8 | 22.3 |
| **2** | $H_{t-Bu}$ | 10.9 | 7.4 |
| | $H_\alpha$ | 10.0 | 5.7 |
| **3** | $H_{t-Bu}$ | 48.1 | 29.3 |
| | $H_\alpha$ | 61.7 | 34.9 |
| | $H_\beta$ | 31.4 | 17.4 |
| | $H_\gamma$ | 24.1 | 11.0 |
| **4** | $H_{t-Bu}$ | 2.8 | 2.0 |
| | $H_\delta$ | 1.7 | 1.4 |
| | $H_\gamma$ | 3.0 | 2.3 |
| | $H_\alpha$ | 10.0 | 8.5 |
| **5** | $H_{t-Bu}$ | 3.2 | 1.8 |
| | $H_\alpha$ | 2.4 | 3.5 |
| | $H_{\gamma ec.}$ | 3.8 | 4.1 |
| | $H_{\beta,\delta ec.}$ | 2.1 | 2.8 |
| | $H_{ax.}$ | 2.1 | 3.3 |

### *Molecular dynamics simulations*

All studied guests studied were systematically subjected to theoretical conformational analysis. Their conformational energy surface was covered by driving all the rotatable torsion angles using the standard two-bond drive technique. The most stable conformer of each guest was considered to be included in the host cavity since significant changes in the conformer population when complexing with the host are not expected.[13]

Each complex was object of several molecular dynamics simulations. Six runs were carried out for each substrate. Productive runs (1000 ps) were preceded by 30 ps of heating to 298 K, and 100 ps for equilibration at this temperature. Two different orientations (**A** and **B**) and three different locations of guest around the host (at the narrower, central or wider zone of the cavity) were used as starting points for a better covering of the configurational phase space. No solvent model was included into the simulations because our focus was the geometry after the inclusion. Three distances between the carbonyl carbon of the guest and three different glycosydic oxygens were restrained using a flat bottom restraint with a tolerance of ±2 Å to prevent the guest from exiting the host cavity.

(13) Sánchez-Ruiz, X.; Ramos, M.; Jaime, C. *J. Mol. Struct.* **1998**, *442*, 93.

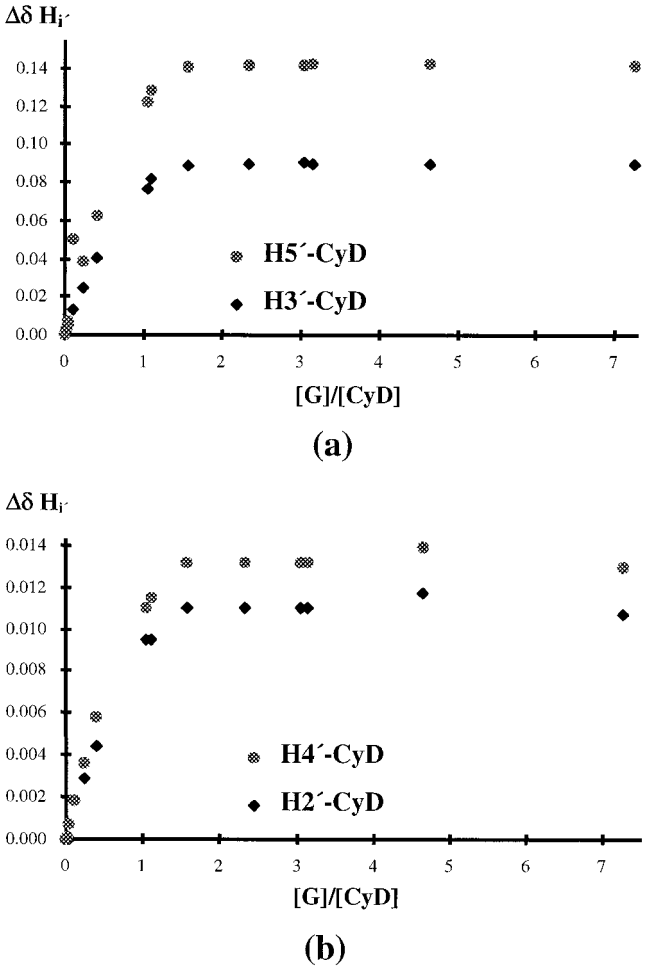


**Figure 4.** Plot for $\Delta\delta$ $H_i$ of complex **1**/*β*-CyD: (a) inner *β*-CyD protons ($H_{3'}$, and $H_{5'}$); (b) outer *β*-CyD protons ($H_{2'}$, and $H_{4'}$).

Computational results were analyzed (energy, geometry, and comparison between experimental NOEs and calculated 'effective distances' for equivalent protons). The energy analysis indicates that both orientations **A** and **B** are equally stable. Computed energy differences were small (from 1 to 4 kJ/mol) and always within the standard deviation of the MD simulations (10−12 kJ/mol).

A geometrical analysis was performed of the MD trajectories corresponding to the last 1000 ps of each simulation making a total of 3000 ps. Figure 7 shows these results by simplified drawings, where guests are represented by two points: the quaternary C atom of the *tert*-butyl group and the C atom at the opposite end of the molecule. Complex **1**/*β*-CyD usually presents the phenyl group included into the CyD cavity either in orientation **A** or **B**. In contrast, the *tert*-butyl group of **1** is less deeply included, and often is located outside the host cavity. Orientation **B** allows the guest to move more freely. Complex **2**/*β*-CyD shows greater mobility and the guest is dispersed within the host cavity; however, the *tert*-butyl group can be considered to be preferentially included although no preference for any orientation can

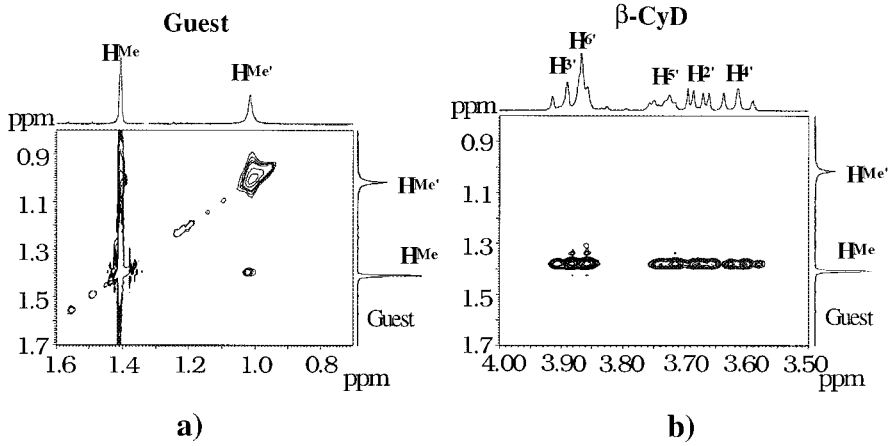


**Figure 5.** Partial 2D-ROESY spectra for complex **1**/*β*-CyD: (a) part for the *tert*-butyl group; (b) interaction *tert*-butyl/host.

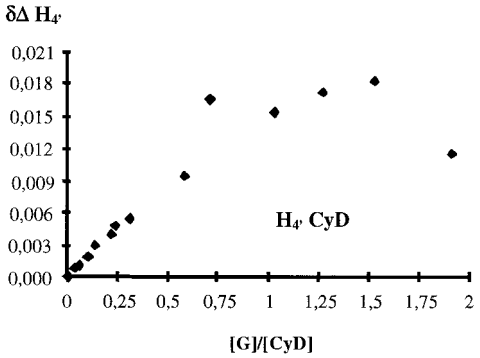


**Figure 6.** Plot of $\Delta\delta$ vs [guest]/[host] for the $H_{4'}$ *β*-CyD protons in complex **5**/*β*-CyD.

**Table 3. Association Constants (*K*) for the Inclusion Complexes between *β*-Cyd and Compounds 1−5 as Obtained Using Program EQNMR and the Data from Our NMR Spectra**

| | *K* from EQNMR | | |
|---|---|---|---|
| guest | $H_{3'}$ | $H_{5'}$ | guest protons |
| **1** | 18301 ± 52 | 6238 ± 53 | 12608 ± 189 |
| **2** | 343 ± 10 | 133 ± 16 | 336 ± 107; 64 ± 7 |
| **3** | 1399 ± 18 | 1432 ± 35 | 1329 ± 128; 1600 ± 3; 179 ± 52 |
| **4** | 9389 ± 67 | 4140 ± 33 | 15376 ± 2453;177408n ± 46; 5523 ± 368; 888 ± 15 |
| **5** | 11586 ± 58 | 10197 ± 48 | 12024 ± 111; 23881 ± 3438; 13346 ± 66 |

be deduced. Simulations on orientation **A** for complex **3**/*β*-CyD present many structures with the *tert*-butyl group located at the narrower part of the cavity, always included, and the propyl group partly on the outside. Orientation **B** is more scattered but the *tert*-butyl group is often outside the cavity. Computations on complex **4**/*β*-CyD indicate a competition between functional groups for inclusion. There are about the same number of ps with complexes of type **A** and **B**, and in both orientations the guest is almost fixed. In contrast, complex **5**/*β*-CyD shows a clear preference for the inclusion of the cyclohexyl group in both complexes. The cyclohexyl group is always inside *β*-CyD in orientation **A** (see Figure 7). Many structures of orientation **B** present the cyclohexyl group inside the wider part of the cavity with the *tert*-butyl group in the narrower part; the inclusion of the *tert*-butyl group in the cavity in this orientation forces the cyclohexyl group outside the cavity.

Our final goal is to compare experimental distances (deduced from experimental NOE values) with computed

**Table 4. Association Constants (*K*) for the Inclusion Complexes between *β*-Cyd and Compounds 1−5 as Obtained Using Program CALCK and the Data from Our NMR Spectra**

| guest | *K* from CALCK | protons considered |
|---|---|---|
| **1** | 3188 | $H_m$ |
| | 38 | $H_o$ |
| | 206 | $H_p$ |
| | 111 | $H_{t-Bu}$ |
| **2** | 1246 | $H_{3'}$, and $H_\alpha$ |
| | 241 | $H_{3'}$ |
| **3** | 10289 | $H_{3'}$, and $H_{5'}$ |
| | 6407 | $H_{3'}$ |
| | 7017 | $H_{5'}$ |
| **4** | 1692 | all guest protons |
| | 1409 | all protons except $H_{5'}$ |
| | 7124 | $H_{3'}$ |
| **5** | 988 | $H_{3'}$ |
| | 719 | $H_{5'}$ |
| | 80 | $H_{3'}$, $H_{5'}$, and all guest protons |
| | 1804 | all guest protons |

interatomic distances to obtain the most probable geometry for inclusion complexes. The well-known dependence[14] of NOE on $(R_{ij})^{-6}$ allows one to obtain experimental distance ratios by simply dividing NOE values: $(\eta_{ab}/\eta_{bc}) = (R_{ab}/R_{bc})^{-6}$. However, when in the studied system several equivalent protons (i.e., seven in the *β*-CyD) exist, the use of "effective" distances is needed. "Effective" distances are those averaged taking into account all the equivalent protons giving rise to one NOE signal. Those distances are obtained by Bendall's equation[15] (eq 1) originally deduced to account for the rotamers contribution:

$$1/R_{\text{eff}}^6 = 1/n \sum(1/R_i^6) \quad (n = 7) \qquad (1)$$

The final "effective" distance was computed by considering all collected samples from the last equilibrated 1000 ps. Experimental NOEs are only observed between nuclei less than 3.5 Å apart. Therefore, computed inter-proton distances greater than 4 Å were discarded. The ratios between "effective" distances were compared with the ratio between corresponding experimental NOEs.

Each molecule presents one set of experimental NOE ratios, which were compared with the computed "effec-

(14) Neuhaus, D.; Williamson, M. P. *The Nuclear Overhauser Effect in Structural and Conformational Analysis*; VCH Publishers Inc.: New York, 1989.

(15) Pegg, D. T.; Bendall, M. R.; Droddell, M. R. *Aust. J. Chem*. **1980**, *33*, 1167.

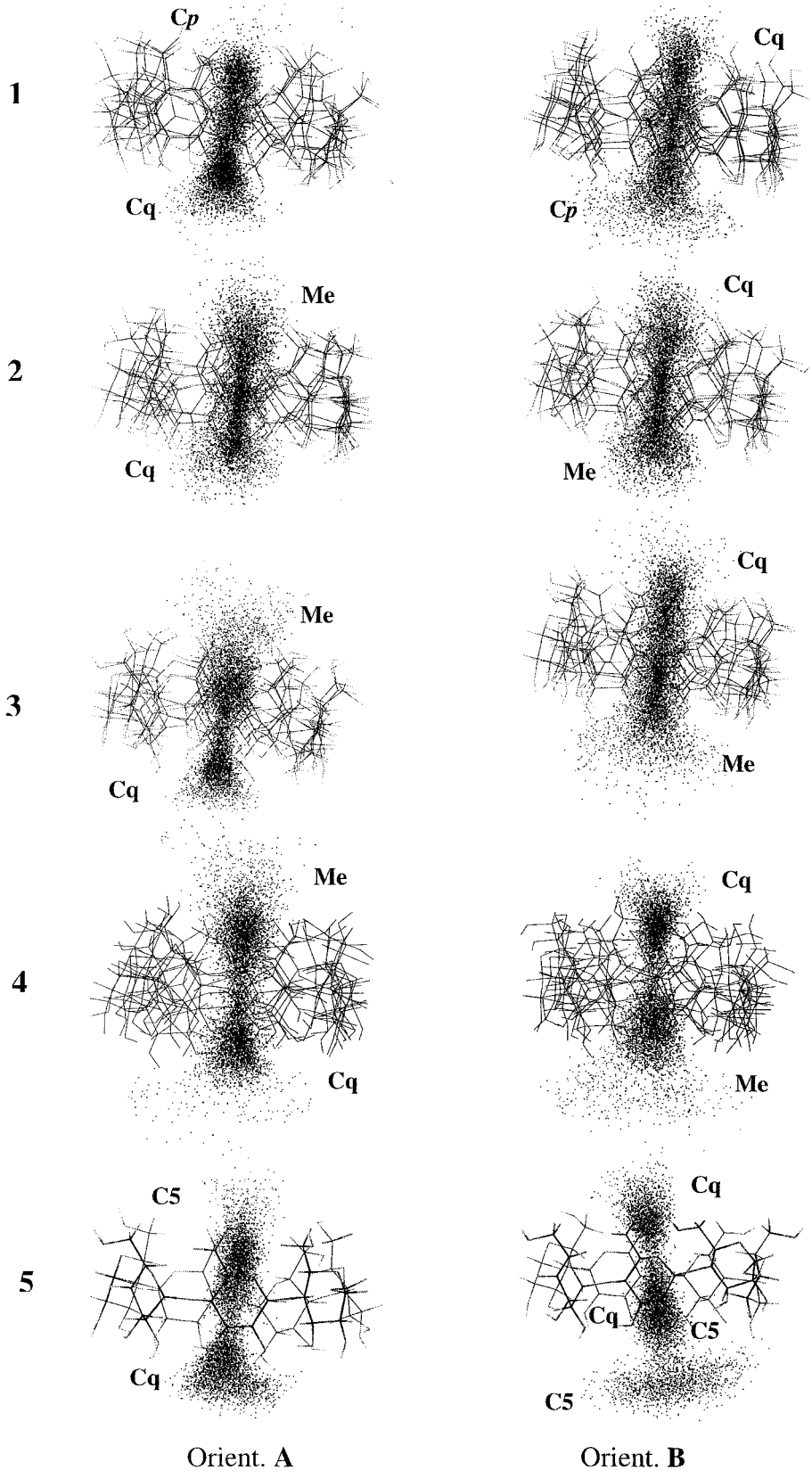


**Figure 7.** Simplified plots of the MD trajectories for complexes of compounds **1**−**5** with $\beta$-CyD. Guests are represented by two points: the quaternary C of the *tert*-butyl group (Cq) and the C atom at the opposite end of the molecule (C*p*, Me, Me, Me, and C5, respectively).

tive" distance ratios coming from the MD runs. Consequently, three comparisons were made: with orientation **A**, with orientation **B** and with both together (**A**+**B**). Table 5 contains the results from these comparisons together with the most probable orientation deduced from the experimental NOE values (vide supra).

Experimental NOE ratios for **1**/$\beta$-CyD correlate (rms = 0.14) with the computed distances in orientation **B**,

**Table 5. Root-Mean-Square (rms) Values for the Comparison of Ratios between Experimental NOE Values and Computed "Effective" Distances Obtained from MD Simulations over Orientation A, B, and A + B (See Text for a Better Explanation)**

| compd | orient. **A** | orient. **B** | orient. **A** + **B** |
|---|---|---|---|
| **1** | 0.27 | 0.14 | 0.17 |
| **2** | 0.05 | 0.06 | 0.06 |
| **3** | 0.24 | 0.13 | 0.19 |
| **4** | 0.09 | 0.22 | 0.08 |
| **5** | 0.19 | 0.26 | 0.00 |

suggesting this orientation as the most probable. Consideration of **A**+**B** orientations also gives a reasonable rms (0.17).

Complex **2**/*β*-CyD correlates with all orientations (rms always <0.1). This is an indication of the large mobility of this guest inside the host cavity. This mobility is also observed when the MD trajectory is analyzed geometrically (see Figure 7).

Complex **3**/*β*-CyD has similar behavior to compound **1**. The "effective" distance analysis indicate that orientation **B** is preferred (rms = 0.13) although the consideration of both orientations produces a reasonable agreement with experimental NOEs (rms = 0.19).

Complexes **4**/*β*-CyD and **5**/*β*-CyD behave similarly. Both complexes present better agreement when both orientations are considered (**A**+**B**). The improvement in the rms is significant in the case of **5**, but slight in the case of **4** (see Table 5).

## Discussion

It is usually considered that the formation of *β*-CyD complexes produces exclusively bimodal inclusion complexes due to the low polarity and low solubility in water of the substrates. However, a careful study of $\Delta\delta$ for all *β*-CyD protons showed the movement of the external protons, indicating some kind of host/guest interaction but on the external wall. The observed shifts for external protons could also be the result of changes in the conformation of the glucose units. However, *J* values for all *β*-CyD protons remain almost unchanged when the host/guest ratio was modified. The largest observed variation was 0.6 Hz (value within the experimental error limit) for $H_{1'}$ in the **1**/*β*-CyD complex when host/guest ratio was changed from 126.6 to 0.52. In addition, *β*-CyD is described[16] as a rather rigid structure due to the hydrogen bonds between secondary hydroxyl groups of neighboring glucose units.

Although program CALCK[10c] was designed for dealing with a single 1:1 complexation, it was used to determine an apparent association constant (*K*), and only a qualitative comparison was performed. Computed Ks do not follow the expected trend (increasing *K* with the size and branching of substituents). We thus conclude that the *tert*-butyl group is better included into *β*-CyD than methyl, propyl and butyl groups, but similar to cyclohexyl, and worse than phenyl group. These conclusions were corroborated by the 2D-ROESY experiments. These results are opposite to those obtained by other researchers with *γ*-CyD as host.[8] The smaller cavity size for *β*-CyD in comparison with *γ*-CyD seems to fit better the phenyl than the cyclohexyl group.

The comparison of the geometrical analysis (Figure 7) and the agreement between NOE values and "effective" distance ratios (Table 5) indicates that experimental results agree better with the calculated interproton distances in the orientation where the guest is less mobile, i.e, orientation **A**. Nevertheless, experimental results are much better explained when both orientations **A** and **B** are considered, which indicates the presence of bimodal complexes.

## Conclusions

Only internal complexation has been observed between *β*-CyD and substrates containing medium polar groups, like *tert*-butyl ketones; nevertheless, these compounds form bimodal complexes. The combination of experimental NOE values and MD simulations has allowed us to study the geometry of the inclusion complexes of these *tert*-butyl ketones. This study indicates the following: (i) the inclusion of a phenyl group into a *β*-CyD seems to be preferred over that of a *tert*-butyl (in agreement with other published results); (ii) inclusion of the *tert*-butyl group is preferred over that of methyl and propyl, although it is very similar to that of an *n*-butyl (at least in *β*-CyD); and (iii) the *tert*-butyl and cyclohexyl groups have very similar preference for their inclusion in *β*-CyD.

## Experimental Section

*tert*-Butyl phenyl ketone, **1**, and pinacolone, **2**, were obtained from Aldrich, while *β*-CyD was obtained from LAISA, and all were used without further purification. Substrates, **3** and **4**, were prepared as described in the literature.[17,18] Compound **5** was prepared in a 63% yield by the same method with slight modifications.

**NMR Experiments.** Complexation was monitored by recording $^1$H NMR spectra for fourteen samples with variable host/guest ratios (standard ranges are from 20 to 0.05, although some arrived to 326 depending on the substrate solubility in water). *β*-CyD was used as a saturated solution in $D_2O$ ($1.63 \times 10^{-2}$ $M^{-1}$). The *β*-CyD anomeric proton ($H_{1'}$) was used as internal reference throughout since it is the less affected by the complexation, and the signal for water is too wide. The host/guest ratio corresponding to each sample was deduced from direct integration of the NMR signals. Samples used for the ROE experiments had concentrations of $10^{-2}$–$10^{-4}$ $M^{-1}$ to prevent false signals coming from general proximity between host and guest.

The NMR spectra were obtained on a 400 MHz spectrometer at 300 K. Cross-relaxation was achieved using a low-power off-resonance continuous-wave irradiation (2.5 kHz) during 600–800 ms as a mixing time. Mixing times giving the maximum NOE value were obtained with the dpfgeno sequence by plotting the observed NOE against the mixing time used. 2D-ROESY spectra were acquired with 32 scans using a relaxation period of 2 s.

**Acknowledgment.** Financial support was obtained from DGES (project PB96-1181). Dr. T. Parella and Prof. A. Virgili are gratefully thanked for helpful comments and suggestions on the NMR experiments. The "Servei de Ressonància Magnètica Nuclear" of the UAB is thanked for allocating spectrometer time.

JO0006021

(16) Szejtli, J. *Chem. Rev.* **1988**, *98*, 1743.

(17) Heathcock, C. H.; Lampe, J. *J. Org. Chem.* **1983**, *48*, 4333.

(18) Corey, E. J.; Suggs, W. J. *Tetrahedron Lett.* **1975**, 2647.